



Cite this: *Sustainable Food Technol.*,  
2023, 1, 762

Received 28th July 2023  
Accepted 29th August 2023

DOI: 10.1039/d3fb00117b

rscl.li/susfoodtech

## Deltamethrin and fenvalerate in vegetables and rice†

Foziya Yusuf Vadia, Jinet Susan Johny, Naved I. Malek   
and Suresh Kumar Kailasa \*

Deltamethrin (DLM) and fenvalerate (FV) are synthetic pyrethroid type II insecticides. Herein, we developed a facile sustainable analytical approach for the detection of DLM and FV using green-fluorescent carbon dots derived from *Moringa oleifera* (MO-CDs) via acid carbonization. The as-synthesized MO-CDs exhibited emission at 524 nm upon excitation at 418 nm with a high quantum yield of 42%. The changes in the intensity of MO-CDs realized two independent calibration graphs for the detection of DLM (0.1 to 100  $\mu\text{M}$ ) and FV (0.5–120  $\mu\text{M}$ ), with limits of detection (LODs) of 0.04 and 0.26  $\mu\text{M}$  for DLM and FV, respectively. This approach was successfully applied to detect DLM and FV in vegetable and rice samples.

### Sustainability spotlight

This work deals with the development of a sustainable analytical method for the detection of two pyrethroids (deltamethrin (DLM) and fenvalerate (FV)) in vegetables and rice using green-fluorescent “MO-CDs” derived from *Moringa oleifera* via acid carbonization. The green-fluorescent MO-CDs exhibited specific functional groups, showing an emission peak at 524 nm when excited at 418 nm with a high quantum yield of 42%. The as-prepared MO-CDs were utilized as a sustainable fluorescent probe for the detection of two pyrethroids (DLM and FV), showing good linear detection ranges for DLM (0.1–100  $\mu\text{M}$ ) and FV (0.5–120  $\mu\text{M}$ ) with limits of detection of 0.04  $\mu\text{M}$  and 0.26  $\mu\text{M}$ , respectively. The amounts of DLM and FV in vegetables and rice samples were thus successfully estimated using the green-fluorescent MO-CDs as a sustainable probe. The green-emissive MO-CDs were synthesized without the use of any toxic chemicals and the prepared MO-CDs are not in toxic nature, which suggests that the MO-CDs could be used as a sustainable fluorescent probe for sensing DLV and FV in food samples.

## 1. Introduction

Insecticides are excessively used in agriculture, industries, medicine, and households for controlling various insects. Insecticides are considered a key factor behind the twentieth-century expansion in agricultural yield; however, they represent a significant toxic risk to humans and can also destroy the food chain.<sup>1</sup> Further, there are many beneficial microorganisms that play a crucial role in enhancing crop productivity, such as rhizobium, acetobacter, azospirillum, phosphorus-solubilizing bacteria, mycorrhizal fungi, and *Bacillus thuringiensis*, but some insecticides can also have indirect effects on these useful microorganisms, particularly those that are soil-dwelling or associated with plant roots.<sup>2,3</sup> Some common insecticides, such as organophosphates, pyrethroids, neonicotinoids, and carbamates, are frequently encountered in agricultural and residential settings. Deltamethrin (DLM) and fenvalerate (FV) are toxic synthetic pyrethroid type II insecticides that are widely used to

kill a number of insects (ants, fleas, spiders, pantry pests, ticks, hemitera, lepidoptera, coleoptera, and other larvae) by attacking their central and peripheral nervous system.<sup>4–6</sup> They are also relevant to the prevention and control of insects in vegetables, cotton, corn, tea, fruit trees, and other crops. Simultaneously, both are persistent in the soil and their degradation takes long time due to the presence of various functional groups that become prominent after their degradation by binding with other organic matter in the environment. Both insecticides are extremely toxic and represent a serious threat to other non-target species, such as honeybees, silkworms, fishes, and other aquatic life.<sup>7,8</sup> The extensive utilization of DLM and FV during the past years has led to the contamination of many aquatic and terrestrial ecosystems, and represent a risk to human health, whereby they can have serious effects on the immune and endocrine systems, the central nervous system, the renal system, the male reproductive system, and increase the risk of breast cancer.<sup>9,10</sup> Hence, monitoring the residual amounts of DLM and FV in the environment is highly demanded in analytical and environmental sciences. In view of this, several analytical techniques have been reported for the detection of both DLM and FV, including gas chromatography,<sup>11</sup> high-performance liquid chromatography,<sup>12</sup> mass spectrometry,<sup>13</sup> immunoassay-based methods,<sup>14</sup> and surface-enhanced

Department of Chemistry, Sardar Vallabhbhai National Institute of Technology, Surat-395 007, Gujarat, India. E-mail: sureshkumarchem@gmail.com; skk@chem.svnit.ac.in

† Electronic supplementary information (ESI) available. See DOI: <https://doi.org/10.1039/d3fb00117b>



Raman spectroscopy.<sup>15</sup> However, these techniques have certain limitations, such as high sample volume, requirement of skilled technicians, time, difficulty, complicated sample preparation, and difficulty to apply for on-site analysis.<sup>16</sup> To overcome these issues, developing a rapid and facile technique for detecting pyrethroids in the environment is highly demanded.

Carbon dots (CDs), also known as carbon quantum dots or C-dots, are a fascinating nanomaterial class that has gained significant attention in recent years. They are small, fluorescent carbon nanoparticles with sizes typically less than 10 nm.<sup>17</sup> CDs have gained significant attention as a highly promising member class among other carbon materials. Their unique “zero-dimensional” point-like structure allows for strong flexibility and diversity, prompting extensive research into their synthesis and application. These nanoscale carbon particles exhibit unique optical and electronic properties, making them highly versatile and suitable for a wide range of applications, including chemobio sensing, biomedicine, catalysis, optoelectronics, and energy.<sup>18,19</sup> Various nanomaterials (nanoclusters, perovskites, nanoparticles) have been used to detect pesticides and other toxic analytes.<sup>20–22</sup> Though, some challenges in their use remain, such as stability, biocompatibility, and toxicity. Hence, in comparison to other analytical techniques, CD-based fluorescence methods have emerged as highly efficient tools for detecting pesticides,<sup>23–25</sup> heavy metal ions,<sup>26,27</sup> biomarkers, and drugs.<sup>28</sup> Despite the promising applications for broad use in pesticide analysis, the advancement of optical sensors utilizing CDs technology still faces challenges, like the quantum yield (QY), fluorescence performance, development of green synthesis methods, purification process, modification in the synthesis methods to tune the optical properties, large-scale production, and real-life applications. So, future research should concentrate on devising new sustainable synthetic approaches by incorporating effective purification techniques for large-scale production and by constructing a comprehensive performance evaluation system. Moreover, it is necessary to transition the production of analytical devices that utilize CDs from research laboratories to real-life applications. This shift would increase the practical utilization of these devices. These efforts would enable the establishment of diverse and robust optical sensing systems for target analytes.<sup>29,30</sup>

In this study, green-fluorescent carbon dots were fabricated from *Moringa oleifera* (as the precursor) (MO-CDs) using phosphoric acid ( $H_3PO_4$ ) as a doping agent and were then used as a probe for sensing DLM and FV in food samples. The acidic conditions obtained due to  $H_3PO_4$  led to a dehydration reaction of the MO, which is a fast-growing, drought-resistant tree that is native to the Indian subcontinent, promoting the carbonization of the phytochemicals (flavonoids, phenolic acid, alkaloids, steroids, saponins, glucosinolate, and terpenes) in the MO and resulting in the formation of CDs.<sup>31</sup> These phytochemicals are enriched with different organic functional groups, so the surface of the synthesized MO-CDs contained various active functional groups, such as –OR, –COR, and –NH. A fluorescent MO-carbon dots-based sensor was developed here for the sensing of DLM and FV, and displayed good linear concentration range responses for DLM (0.1 to 100  $\mu M$ ) and FV (0.5–120  $\mu M$ ) with LODs of 0.04  $\mu M$  and 0.26  $\mu M$ , respectively. The selectivity study revealed that the MO-CDs probe

did not exhibit selectivity towards other pesticides. Lastly, the as-synthesized MO-CDs were effectively used for an assay for DLM and FV in vegetables and rice, displaying a good recovery response.

## 2. Experimental section

### 2.1. Chemicals

*Moringa oleifera* (drumsticks) were collected from the local market, in Surat, Gujarat, India. All chemicals used for the experiment were of analytical grade. Imazethapyr, thiamethoxam, isoproturon, pyriithiobac sodium, imidacloprid, and metalaxyl were collected from Atul, Ankleshwar. DLM, cypermethrin, FV, indoxacarb, clodinafop, and lambda-cyhalothrin were obtained from Gujarat Insecticides Ltd Ankleshwar. Thiachloprid and fipronil were received from Crop Life Science Ltd. Pendimethalin was obtained from Cheminova India Limited, India. The chemicals  $Ni(SO_4)_2$ ,  $Cr(NO_3)_3$ ,  $Zn(NO_3)_2$ ,  $Cd(NO_3)_2$ ,  $CoCl_2$ , KBr,  $Na_2SO_4$ ,  $MnCl_2$ ,  $Mg(NO_3)_2$ ,  $AlCl_3$ , NaOH, ethanol, and  $H_3PO_4$  were bought from Sigma-Aldrich. The Milli-Q purification system was utilized to obtain ultrapure water.

### 2.2. Instrumentation

Various analytical instruments were employed to characterize the pre-synthesized *Moringa oleifera*-derived CDs. The emission spectra of the MO-CDs were recorded using a Cary Eclipse spectrophotometer (Agilent Technologies, USA), while the UV absorption study was conducted using a Maya Pro 2000 spectrophotometer (Ocean Optics, USA). Fourier transform infrared spectrometry (FT-IR) (APHA II, Bruker, Germany) was used to measure the surface functionalities of the MO-CDs. Transmission electron microscopy (TEM; JEM 2100, JEOL Japan) was used for determining the average size of the MO-CDs. The surface charge and hydrodynamic diameter of the MO-CDs were analyzed using a Horiba SZ-1000 system.

### 2.3. Synthesis of the MO-CDs

The *Moringa oleifera* (drumsticks) samples (50 g) were cleaned with water, peeled, and then the seeds were removed. The peeled drumsticks were chopped and stored at  $-20\text{ }^\circ\text{C}$  in the freezer. The green-coloured CDs were synthesized by the modification of a described method in the literature.<sup>32</sup> First, 3.0 g of frozen, chopped drumsticks and 10 mL of 40 N  $H_3PO_4$  that were used to fabricate the MO-CDs were mixed and then sonicated for 15 min, followed by heating the solution for 40 min at  $90\text{ }^\circ\text{C}$ . The resulting brownish crude solution was filtered and neutralized with sodium hydroxide (1.0 N). The as-prepared MO-CDs were stored at  $-3\text{ }^\circ\text{C}$ . Scheme 1 in the ESI† provides a schematic of the synthesis process for the MO-CDs.

### 2.4. Sensing of deltamethrin and fenvalerate

To carry out the fluorescence sensing of DLM and FV in a typical experiment, stock solutions of different pesticides were prepared (metalaxyl, pyriithiobac sodium, imazethapyr, isoproturon, thiamethoxam, DLM, and FV, all at 1.0 mM). Next, 0.5 mL of these pesticide solutions were transferred to separate 4 mL glass vials containing 1.0 mL of MO-CDs and vortexed for



2 min. After vortexing, the vials were set aside for 1 min before conducting fluorescence spectral measurements. Further, to assess the selectivity of as-synthesized MO-CDs towards DLM and FV, several interfering pesticides, including cypermethrin, thiacloprid, indoxacarb, fipronil, pendimethalin, imidacloprid, clodinafop, and  $\lambda$ -cyhalothrin, were tested. The changes in emission intensity against various concentrations of DLM and FV were compared through calibration graphs.

## 2.5. QY measurement

The QY of the MO-CDs was calculated with consideration of the reference sample quinine sulfate (QS) compound using the following equation.

$$Q_{\text{MO-CDs}} = Q_{\text{QS}} \times (I_{\text{MO-CDs}}/I_{\text{R}}) \times (\eta_{\text{MO-CDs}}^2/\eta_{\text{R}}^2) \times (A_{\text{R}}/A_{\text{MO-CDs}})$$

where  $Q_{\text{MO-CDs}}$  represents the QY of the MO-CDs,  $Q_{\text{QS}}$  is the QY of QS as the reference ( $Q_{\text{QS}} = 54.6\%$ ), “ $I$ ” represent the integrated area of the emission peaks of the MO-CDs and QS, “ $\eta$ ” signifies the refractive index of the MO-CDs and QS, subscript “R” denotes the reference sample “QS”, and “A” is the absorbance of both the MO-CDs and QS. The QY of the MO-CDs was calculated as 42%.

## 2.6. Assessment of deltamethrin and fenvalerate recovery in real samples

The as-prepared MO-CDs were applied to quantify DLM and FV amounts in cabbage, corn, and rice as real samples. The vegetables (cabbage and corn) were bought from a nearby shop and employed with no further treatment. The cabbage and corn were cleaned and finely chopped using a stainless-steel knife. The samples (cabbage, 1.5 g) were spiked with different concentrations of DLM (0.1, 0.25, 0.5, and 1.0  $\mu\text{M}$ ) and FV (0.5, 1.0, 2.5, and 5.0  $\mu\text{M}$ ), and then put aside overnight. Then, a 1 : 1 ratio of acetonitrile and water was added to the spiked sample and the solution was sonicated for 15 min. The resulting solution was filtered using Whatman filter paper-292 and then the spectra were measured by introducing them into MO-CDs solutions. Further, DLM (0.1, 0.25, 0.5, and 1.0  $\mu\text{M}$ ) and FV (0.5, 1.0, 2.5, and 5.0  $\mu\text{M}$ ) were spiked into 1.5 g of corn and put in the dark overnight. After that, a 1 : 1 ratio of methanol and water was added to the sample, and filtered, followed by sonication. For the rice sample, 10 g of rice powder was spiked with different concentrations of DLM and FV and put in the dark for 24 h. The extract was obtained using a 1 : 1 ratio of methanol and water followed by sonication. The resulting solution was filtered using Whatman filter paper and then the amounts of DLM and FV were estimated by the described procedure earlier using the MO-CDs as a sensor and fluorescence spectrometry.

# 3. Results and discussion

## 3.1. Characterization of the MO-CDs

Here, *Moringa oleifera* (drumsticks) was used as a green carbon precursor to fabricate MO-CDs using  $\text{H}_3\text{PO}_4$  treatment. Under

365 nm UV light, the as-synthesized MO-CDs exhibited green-coloured fluorescence and appeared yellowish in daylight. In order to measure the optimum emission peak of the MO-CDs, the emission spectra of the MO-CDs were recorded at different excitation wavelengths ranging from 380 to 450 nm (Fig S1a and b of the ESI†). The fluorescence spectrometer detected the highest emission at 524 nm when excited at 418 nm. The UV-visible, excitation, and emission spectra of the MO-CDs were measured and displayed  $\lambda_{\text{max}}$  at 325 nm and  $\lambda_{\text{Em/Ex}}$  at 524/418 nm (Fig. 1a). Meanwhile, upon excitation of the MO-CDs at 418 nm, the Commission Internationale de l'Éclairage (CIE) was used to confirm the colour region coordinates of the MO-CDs, demonstrating that for the as-prepared MO-CDs these lay in the green region (0.29, 0.59) (Fig. 1b). The stability of the MO-CDs was confirmed by examining the emission spectra at different time intervals (1–80 days), which indicated that the synthesized MO-CDs were stable for up to 10 days without significant change in the emission intensity (Fig. S2a of the ESI†); however, after 10 days, the emission signals slightly decreased. These results confirm that the as-synthesized MO-CDs could be used as a probe for sensing and bioimaging applications. Moreover, the stability of the MO-CDs was also studied by exposing the MO-CDs to UV

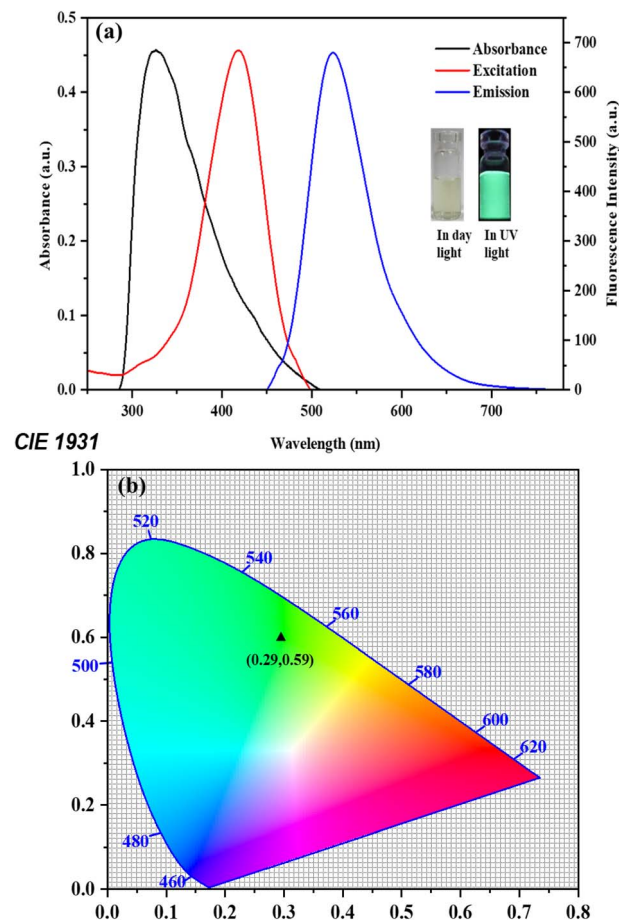


Fig. 1 (a) UV-visible absorbance, fluorescence excitation (418 nm), and emission (524 nm) spectra of the MO-CDs; (inset): images of the MO-CDs captured in daylight and under UV light (365 nm). (b) CIE colour coordinates of the green-fluorescent MO-CDs.



light at 365 nm, which indicated that the MO-CDs strongly emitted green fluorescence even after exposure to 365 nm UV light for 4 h, and then the green emission only slightly decreased, signifying that the prepared MO-CDs exhibited good photostability, and could be used as optical sensors (Fig. S2b of the ESI†). To examine the repeatability of the method used for the fabrication of the MO-CDs, MO-CDs were synthesized in three different batches under optimum conditions and the emission spectra of the MO-CDs prepared from the different batches were studied, and are shown in Fig S3a–c of the ESI.† The emission spectral characteristics of the MO-CDs demonstrated that the developed method had good reproducibility to generate green-fluorescent MO-CDs without any change in emission spectra, together with good stability for up to 15 days, suggesting that the developed method could be used for the preparation of green-emitting MO-CDs for sensing and bioimaging applications.

The FT-IR spectra were studied to explore the surface functionality of as-fabricated MO-CDs and with both insecticides (Fig. S4 of the ESI†). Broad peaks corresponding to hydroxyl and amino stretching were observed in the spectral range of 3200–3500  $\text{cm}^{-1}$ . A peak for C=N stretching was observed at 1639  $\text{cm}^{-1}$  and a peak of C–H bending was noticed at 1413  $\text{cm}^{-1}$ . The characteristic peaks at 1130 and 1068  $\text{cm}^{-1}$  were attributed to P–O–C bending. The individual peaks at 860 and 953  $\text{cm}^{-1}$  were assigned to P–O and P=O stretching vibrations in the MO-CDs.<sup>33</sup> In order to observe the interaction of the surface functional groups of MO-CDs with target analytes (DLM and FV), the FT-IR spectra of the MO-CDs with DLM and FV were studied and are shown in Fig. S5 of the ESI.† This data revealed that the intensity of the O–H and N–H peaks decreased due to the interaction between the surface functional groups of the MO-CDs and the functional groups of both insecticides. The as-prepared MO-CDs showed a  $\lambda_{\text{max}}$  at 325 nm (Fig. S5 of the ESI†), confirming the presence of  $\pi$ – $\pi^*$  and  $n$ – $\pi^*$  electronic transitions, which were due to the existence of C=C, C=O, C–O, and C=N groups in the MO-CDs. The QY of the green-fluorescent MO-CDs was 42%. Further, to measure the sizes of the MO-CDs, TEM analysis was performed and the resulting images are shown in Fig. 2a and b, displaying that the average size of the as-prepared MO-CDs was  $3.09 \pm 1.06$  nm. The mean hydrodynamic diameter of the MO-CDs was investigated by dynamic light scattering (DLS) and was found to be 3.3 nm, which is slightly higher than the TEM result for the MO-CDs, likely due to one measurement being the hydrodynamic diameter of the MO-CDs (Fig. S6a of the ESI†). Moreover, elemental analysis of the MO-CDs was performed by X-ray photoelectron spectroscopy (XPS) (Fig. 3). Fig. 3a presents the overall survey spectrum of MO-CDs, showing four main peaks for C 1s, O 1s, Na 1s, and P 2p, respectively. The atomic ratios of C 1s, O 1s, N 1s, and P 2p were 42.36%, 48.91%, 0.98%, and 7.76%, respectively. The XPS spectrum of C 1s consisted of two peaks, corresponding to  $\text{sp}^2$  hybridized C in C=C bonds at 284.8 eV and C=O carbon at 288.1 eV, as shown in Fig. 3b. The N 1s spectrum in Fig. 3c of MO-CDs exhibited the presence of  $-\text{NH}_2$  groups at 399.1 eV. The peaks at 530.8 and 535.6 eV corresponded to the binding energy of the O 1s of MO-CDs (Fig. 3d). The P 2p spectrum of MO-CDs exhibited a peak at 132.8 eV (Fig. 3e), corresponding to P–O–C bond.<sup>34,35</sup>

### 3.2. Effect of pH

Generally, CDs can be influenced by pH, and thus to evaluate the effect of pH on the fluorescence sensing of both pesticides using MO-CDs as a probe, phosphate buffered saline (PBS) was here used to check the fluorescence response of the MO-CDs with and without the addition of the pesticides. The impact of PBS buffer on the as-synthesized MO-CDs revealed that the surface of the as-prepared MO-CDs was pH insensitive at pH 2.0–12.0, where due to the inert surface functionality, the intensity of the MO-CDs spectrum was unchanged (Fig. S7a in the ESI†). Next, the fluorescence spectra of MO-CDs were measured with the addition of DLM and FV at various PBS pH of 2.0–12.0, revealing the maximum quenching in the neutral condition in the presence of DLM and FV (Fig. S7b and c of the ESI†), illustrating the degree of fluorescence quenching of the MO-CDs by both pesticides was almost similar with and without PBS pH changes, confirming that the as-prepared MO-CDs could be used for the assaying of both pesticides without any buffer pH. In order to learn more about how salt affects the stability of the as-synthesized MO-CDs, different concentrations of NaCl were added to the MO-CDs, and the emission spectra were measured (Fig. S7d of the ESI†). The results showed that in a high salt environment, the fluorescence intensity of the MO-CDs was constant, confirming that the MO-CDs exhibited good stability in the presence of NaCl, suggesting that the MO-CDs could serve as a promising probe for the sensing of both pesticides in harsh conditions.

### 3.3. Fluorescence sensing of deltamethrin and fenvalerate

The as-prepared MO-CDs were tested with various pesticides (imazethapyr, thiamethoxam, isoproturon, pyriithiobac sodium, metalaxyl, DLM, and FV; all at 1.0 mM) and the spectra were recorded in order to study the sensing application potential of the MO-CDs toward common pesticides (Fig. 4). It was clearly found that the emission intensity of MO-CDs was quenched only with the addition of DLM and FV, indicating that MO-CDs could act as a probe for the detection of both DLM and FV pesticides *via* a fluorescence quenching mechanism. Importantly, the reproducibility of the method was investigated by examining the emission spectra of MO-CDs prepared from three different batches with the addition of both DLM and FV separately (Fig. S3d–f of the ESI†), with the results suggesting that the as-prepared MO-CDs could act as an optical method for the fluorescence sensing of both DLM and FV pesticides with a high degree of reproducibility. Applying various concentrations of DLM (0.1–100  $\mu\text{M}$ ) and FV (0.5–120  $\mu\text{M}$ ), the emission intensities of the as-fabricated MO-CDs were recorded, and are shown in Fig. 5a and b, revealing that the fluorescence quenching was linearly dependent on the increasing concentrations of DLM and FV. Fig. S8a and b in the ESI† show the linear responses between the fluorescence intensity of the MO-CDs and the concentrations of DLM (1–100  $\mu\text{M}$ ) and FV (1–300  $\mu\text{M}$ ), exhibiting correlation coefficients ( $R^2$ ) of 0.9901 and 0.9918 for DLM and FV, respectively. The LODs for DLM and FV were determined to be 0.004  $\mu\text{M}$  and 0.26  $\mu\text{M}$ , respectively. In addition, Tables 1 and 2 provide a comparison between the analytical



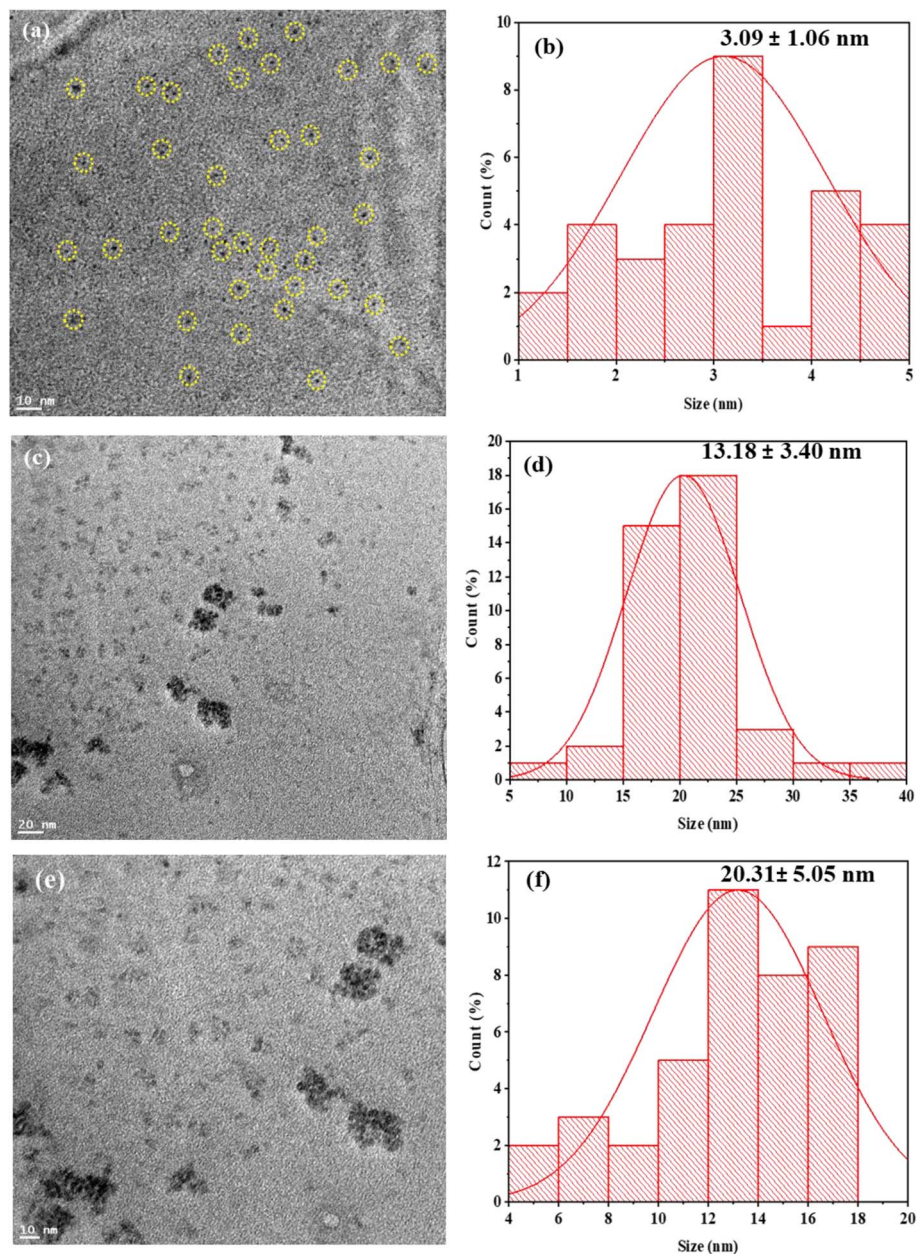


Fig. 2 TEM images of MO-CDs with the target analytes. (a) MO-CDs at 10 nm scale bar, (b) histogram of MO-CDs, and (c) MO-CDs + DLM at 20 nm scale bar and (e) MO-CDs + FV at 10 nm scale bar. Histograms of MO-CDs with (d) DLM and (f) FV.

features of the present method and other traditional analytical techniques for the detection of DLM and FV,<sup>36-50</sup> demonstrating that the MO-CDs-based fluorescence method has good selectivity, and a higher sensitivity than the other reported methods.<sup>40,41</sup> Furthermore, the preparation of the MO-CDs did not require any expensive reagents, suggesting the MO-CDs could be used as a sustainable green-fluorescent probe for the detection of both DLM and FV in food samples.

### 3.4. Sensing mechanism

To confirm the fluorescence quenching of MO-CDs by both DLM and FV, different characterizations were performed (UV-

visible, lifetime, FT-IR, HR-TEM, DLS, and Zeta potential). The absorption spectra of both insecticides (DLM and FV) and the fluorescence spectra of the MO-CDs ( $\lambda_{\text{ex/em}}$ ) were studied (Fig. S9 of the ESI<sup>†</sup>), revealing the absorption spectra of both analytes overlapped (50%) with the fluorescence excitation spectrum of the MO-CDs, suggesting an inner filter effect (IFE) mechanism. The UV-visible spectra of the MO-CDs alone and MO-CDs with DLM and FV showed significant differences, suggesting interactions between the active functional groups of both insecticides (Fig. S5 of the ESI<sup>†</sup>). Lifetime analysis was performed to investigate the decay dynamics of the as-synthesized MO-CDs with both analytes, which showed the average lifetime of the MO-CDs was 1.60 ns. However, this was



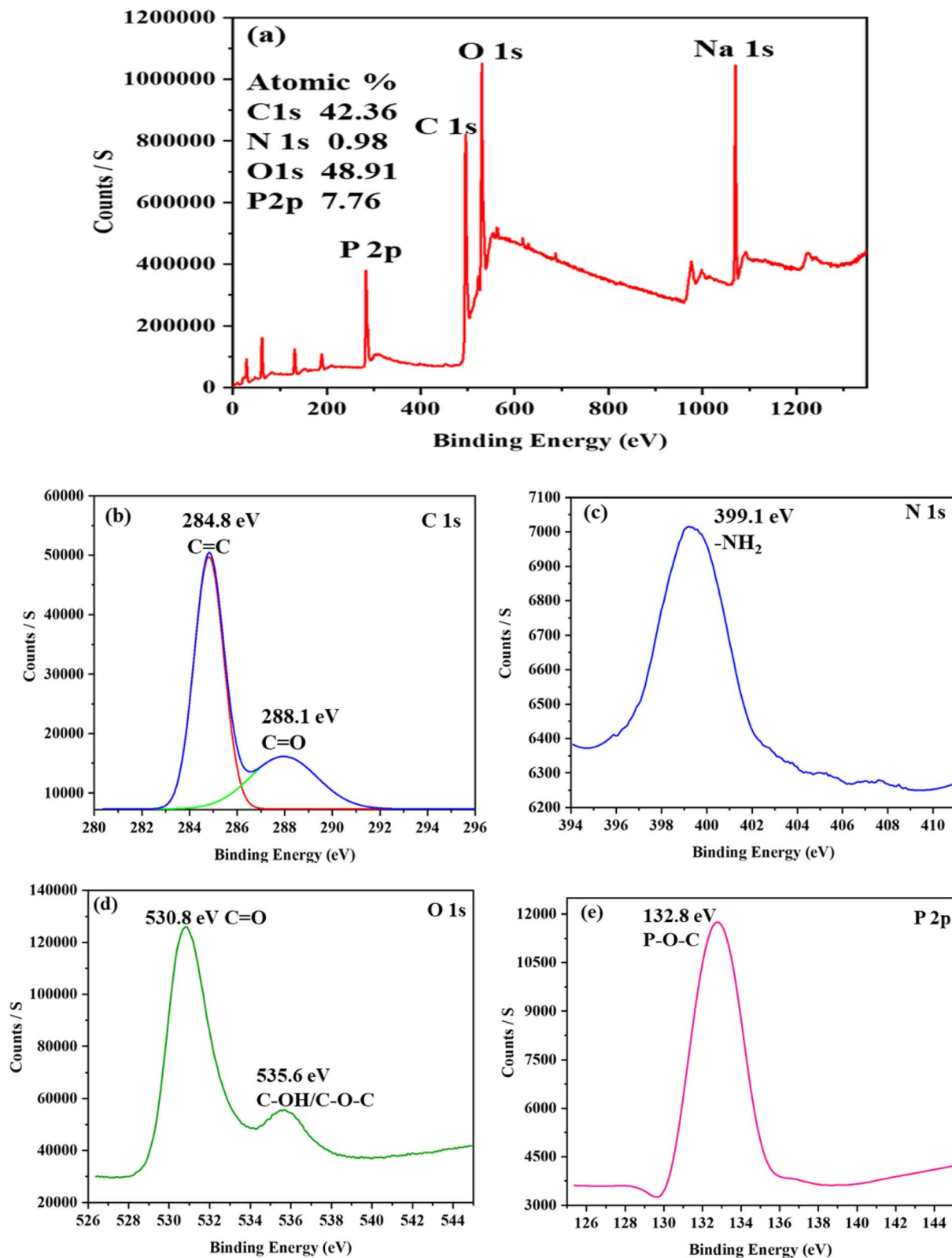


Fig. 3 XPS analysis of MO-CDs. (a) Survey spectrum; high-resolution spectra of (b) C 1s, (c) N 1s, (d) O 1s, and (e) P 2p.

slightly changed in the presence of DLM (2.16 ns) and FV (1.71 ns), indicating a minimal change in the lifetimes upon the interaction of both insecticides (Fig. S10 of the ESI<sup>†</sup>), suggesting

static quenching, where the fluorescence of MO-CDs was quenched by both insecticides in a non-dynamic manner. Moreover, the FT-IR data of the MO-CDs alone and MO-CDs



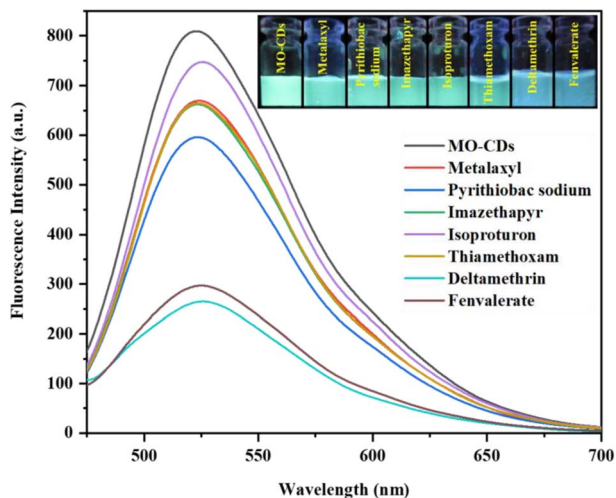


Fig. 4 (a) Emission spectra of MO-CDs at 524 nm upon the addition of different pesticides (imazethapyr, thiamethoxam, isoproturon, pyriithiobac sodium, metalaxyl, DLM and FV; all at 1.0 mM); (inset): picture of the MO-CDs solutions with the above-mentioned pesticides under 365 nm UV light.

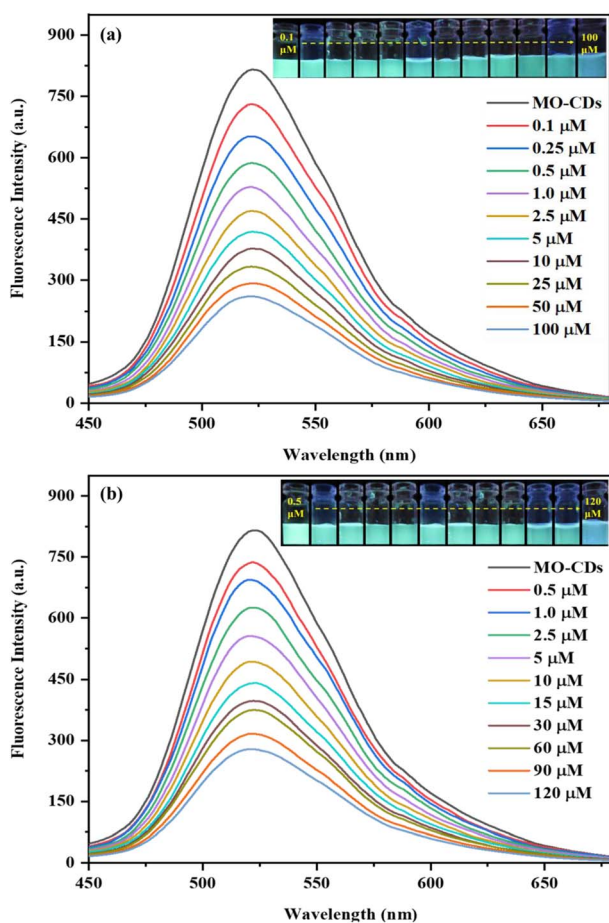


Fig. 5 Emission spectra of MO-CDs with the addition of various concentrations of (a) DLM (0.1–100  $\mu\text{M}$ ) and (b) FV (0.5–120  $\mu\text{M}$ ); (insets): photographs displaying the variations in green fluorescence of the MO-CDs with increasing amounts of both pesticides under UV excitation at 365 nm.

Table 1 Comparison of the proposed fluorescent sensor with other reported analytical methods for the detection of DLM<sup>a</sup>

Analytical method	Linear range ( $\mu\text{M}$ )	Limit of detection ( $\mu\text{M}$ )	Ref.
GC-MS	0.05–1	—	36
Au NPs-MNBT	0.005–1	0.005	37
HPLC	0.0019–0.98	0.0013–0.0029	38
UCNPs@MNPs	0.0019–1.97	0.0014	39
CdTe-SiO <sub>2</sub> -MIPs	0.98–69.27	0.31	40
GQDs	0.59–19.79	0.29	41
S, N-CQDs	0.0035–0.039	0.00059	42
Amylase AuNCs	0.2–0.9	0.006	43
MO-CDs	0.1–100	0.040	This work

<sup>a</sup> GC-MS, gas chromatography/mass spectrometry; AuNPs-MNBT, gold nanoparticles modified with 2-mercapto-6 nitrobenzothiazole; UCNPs@MNPs, upconversion nanoparticle @ magnetic nanoparticles; CdTe-SiO<sub>2</sub>-MIPs, silica molecularly imprinted nanospheres embedded CdTe quantum dots; GQDs, graphene quantum dots; S, N-CQDs sulfur, nitrogen co-doped carbon quantum dots.

Table 2 Comparison of the proposed fluorescent sensor with other reported analytical methods for the detection of FV

Method	Linear range ( $\mu\text{M}$ )	Limit of detection ( $\mu\text{M}$ )	Ref.
HPLC	0.0011–0.47	0.00023	44
GC	0.0016–1.190	0.00047	45
GC	0.0047–4.7	$9.5 \times 10^{-5}$	46
Microfluidic	0.023–2.38	0.007	47
AuNPs	0.0004–0.47	0.0001	48
CdTe QDs@MIPs <sup>a</sup>	—	0.0032	49
SiO <sub>2</sub> @TiO <sub>2</sub> @Ag	0.001–0.1	0.0002	50
MO-CDs	0.5–120	0.26	This work

<sup>a</sup> CdTe QDs@MIPs, CdTe quantum dots modified molecularly imprinted polymer.

with DLM and FV were examined to confirm the interaction between the MO-CDs and both insecticides. The data showed that the stretching vibrations of MO-CDs alone and MO-CDs with DLM and FV were significantly different due to the interaction between the MO-CDs and both insecticides. The morphology of MO-CDs in the presence of both insecticides was verified using HR-TEM analysis (Fig. 2c–f), revealing that the sizes of the MO-CDs noticeably increased ( $13.18 \pm 3.40$  and  $20.31 \pm 5.05$  nm) upon the addition of DLM and FV, respectively. Also, DLS analysis of the MO-CDs with DLM and FV gave sizes of 21.4 and 27.2 nm, respectively, which showed there was a significant increase in the diameter of the MO-CDs (3.3 nm) (Fig. S6b and c of the ESI<sup>†</sup>). In addition, the surface charge of the as-fabricated MO-CDs showed a negative charge of  $-33.4$  mV, which was reduced to  $+2.1$  and  $+8.7$  mV with the addition of DLM and FV, respectively (Fig. S11a–c of the ESI<sup>†</sup>), indicating the occurrence of electrostatic interaction between the MO-CDs and both insecticides. The analytical data presented strongly support that the as-prepared MO-CDs can serve as a fluorescent probe for the simultaneous detection of DLM and FV.



### 3.5. Selectivity study

To examine the selectivity of the MO-CDs toward DLM and FV, the fluorescence spectral characteristics of the MO-CDs were investigated in the presence of other interfering species with and without DLM and FV separately (Fig. 6). Different metal cations ( $\text{Mn}^{2+}$ ,  $\text{Mg}^{2+}$ ,  $\text{Cd}^{2+}$ , and,  $\text{Na}^+$ , 1.0 mM), anions ( $\text{Cl}^-$ ,  $\text{Br}^-$ ,  $\text{NO}_3^-$ , and,  $\text{SO}_4^{2-}$ , 1.0 mM), and pesticides (cypermethrin, thiacloprid, indoxacarb, and, fipronil, 1.0 mM) were studied in the presence and absence of DLM, while for FV, the cations ( $\text{Zn}^{2+}$ ,  $\text{Ni}^{2+}$ ,  $\text{Co}^{2+}$ , and,  $\text{Cr}^{3+}$ , 1.0 mM), anions ( $\text{SO}_4^{2-}$ ,  $\text{NO}_3^-$ ,  $\text{I}^-$ , and,  $\text{Cl}^-$ , 1.0 mM), and pesticides (pendimethalin, imidacloprid, clodinafop, and, lambda-cyhalothrin, 1.0 mM) were tested. The experimental observations indicated that the fluorescence intensity of the MO-CDs was specifically quenched with the addition of DLM and FV but not influenced by the other chemical species present in the experimental conditions, as shown in Fig. 6a and b, and no fluorescence enhancement or

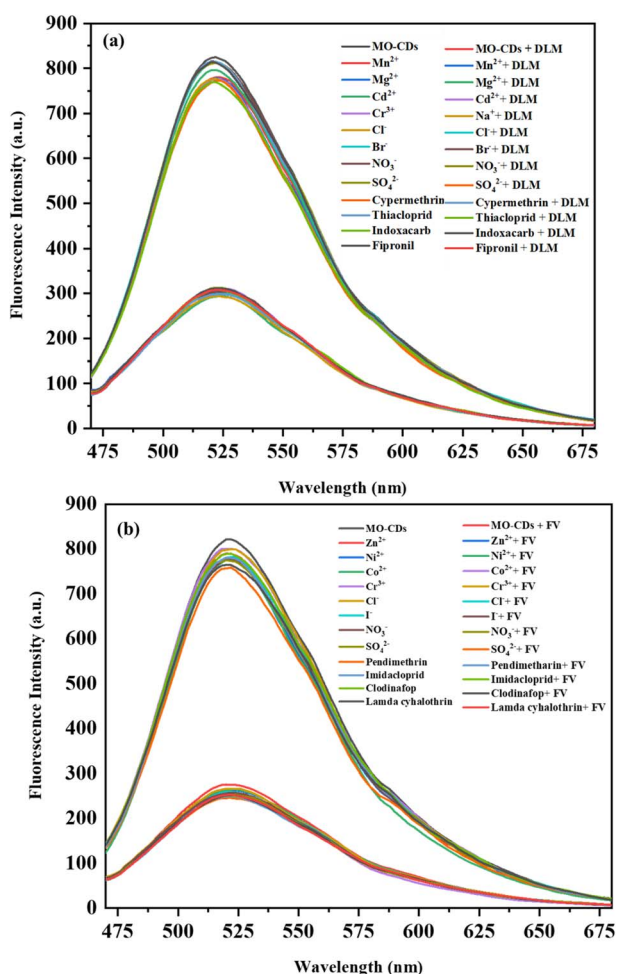


Fig. 6 Emission spectra of the MO-CDs (a) with and without the addition of DLM with different interfering agents of metal cations ( $\text{Mn}^{2+}$ ,  $\text{Mg}^{2+}$ ,  $\text{Cd}^{2+}$ , and,  $\text{Na}^+$ ), anions ( $\text{Cl}^-$ ,  $\text{Br}^-$ ,  $\text{NO}_3^-$ , and,  $\text{SO}_4^{2-}$ ), and pesticides (cypermethrin, thiacloprid, indoxacarb, and, fipronil), and (b) with and without the addition of FV with different interfering agents of metal cations ( $\text{Zn}^{2+}$ ,  $\text{Ni}^{2+}$ ,  $\text{Co}^{2+}$ , and,  $\text{Cr}^{3+}$ ), anions ( $\text{SO}_4^{2-}$ ,  $\text{NO}_3^-$ ,  $\text{I}^-$ , and,  $\text{Cl}^-$ ), and pesticides (pendimethalin, imidacloprid, clodinafop, and, lambda-cyhalothrin).

quenching were observed with the other pesticides. This suggests that the fluorescence response of the MO-CDs is specific to DLM and FV, indicating their potential for the selective detection of DLM and FV. Even in the presence of other pesticides, DLM and FV could quench the intensity of the MO-CDs, implying that DLM and FV can interact with the MO-CDs and effectively quench the fluorescence. In addition, to explore the selectivity of the MO-CDs between DLM and FV, the selectivity of the MO-CDs was studied in the presence of both insecticides using different ratios of DLM and FV (DLM: FV, 100:100, 100:75, 100:50, 100:25, 75:100, 50:100 and 25:100  $\mu\text{M}$ ), and the results are shown in Fig. S12a and b in the ESI,<sup>†</sup> which reveal that the MO-CDs exhibited a higher degree of selectivity toward DLM compared to FV.

### 3.6. Analysis of deltamethrin and fenvalerate in real samples

After studying the sensitivity and selectivity of MO-CDs toward DLM and FV, the effectiveness of the MO-CDs was assessed for detecting DLM and FV in vegetables and rice. To achieve this, the vegetables and rice samples were spiked with different concentrations of DLM (0.1, 0.25, 0.5, and 1.0  $\mu\text{M}$ ) and FV (0.5, 1.0, 2.5, and 5.0  $\mu\text{M}$ ). The extraction and preparation of the samples followed the above-mentioned procedure, and the resulting extracts were appropriately diluted for further analysis. Using this approach, good recoveries were noticed in the range of 96.0–99.0%, with a relative standard deviation (RSD) of 0.03–0.13% for assaying DLM in the vegetables and rice samples (Table S1 of the ESI<sup>†</sup>). Also, the recovery of FV ranged from 95.0–99.0%, with less than two RSD values (Table S2 of the ESI<sup>†</sup>). These findings clearly indicate that the developed green-fluorescent MO-CDs had excellent reliability and accuracy for detecting DLM and FV in vegetables and rice.

## 4. Conclusions

In summary, a green chemistry approach was established to synthesize green-fluorescent MO-CDs from *Moringa oleifera* using  $\text{H}_3\text{PO}_4$  as an oxidizing agent. Upon excitation at 418 nm, the as-prepared MO-CDs emitted green fluorescence at 524 nm. Moreover, the MO-CDs showed a uniform distribution in aqueous solution with an average size of  $1.56 \pm 0.31$  nm. The as-fabricated MO-CDs were utilized as a fluorescent probe for sensing DLM and FV via a turn-off mechanism. The method demonstrated favourable linear detection ranges of 0.1–100 and 0.5–120  $\mu\text{M}$  with LODs of 0.040 and of 0.26  $\mu\text{M}$  for DLM and FV, respectively. The practicality of the probe was confirmed by successfully analyzing DLM and FV in real vegetables and rice samples, showing good recoveries and lower RSD values. Hence, the MO-CDs demonstrated potential as a pesticide fluorescent sensor that could be used as part of a simple sustainable analytical strategy for assaying both pyrethroid pesticides in food samples.

## Conflicts of interest

There are no conflicts to declare.



## Acknowledgements

This work was financially supported by the Department of Science and Technology, Government of India under Women Scientist Scheme-A (DST/WOS-A/CS-77/2021). FYV, NIM and SKK sincerely acknowledge the Director, SVNIT, Surat, India, for providing the necessary infrastructure to carry out this work.

## References

- 1 N. Alvandi, S. Assariha, N. Esfandiari and R. Jafari, Off-on sensor based on concentration-dependent multicolor fluorescent carbon dots for detecting pesticides, *Nano-Struct. Nano-Objects*, 2021, **26**, 100706, DOI: [10.1016/J.NANOSO.2021.100706](https://doi.org/10.1016/J.NANOSO.2021.100706).
- 2 A. Javaid, Beneficial microorganisms for sustainable agriculture, *Genetic engineering, biofertilisation, soil quality, and organic farming*, 2010, pp. 347–369, DOI: [10.1007/978-90-481-8741-6\\_12](https://doi.org/10.1007/978-90-481-8741-6_12).
- 3 I. C. Yadav and N. L. Devi, Pesticides classification and its impact on human and environment, *Environ. Sci. Eng.*, 2017, **6**, 140–158.
- 4 S. Tuck, A. Furey, S. Crooks and M. Danaher, A review of methodology for the analysis of pyrethrin and pyrethroid residues in food of animal origin, *Food Addit. Contam.*, 2018, **35**, 911–940, DOI: [10.1080/19440049.2017.1420919](https://doi.org/10.1080/19440049.2017.1420919).
- 5 H. Zhan, Y. Huang, Z. Lin, P. Bhatt and S. Chen, New insights into the microbial degradation and catalytic mechanism of synthetic pyrethroids, *Environ. Res.*, 2020, **182**, 109138, DOI: [10.1016/J.ENVRES.2020.109138](https://doi.org/10.1016/J.ENVRES.2020.109138).
- 6 J. Liu, Q. Zhang, W. Zhang, X. Ding, X. Hu, F. Zhao and P. Li, Development of a fluorescence-linked immunoassay based on quantum dots for fenvalerate, *Food Agric. Immunol.*, 2014, **25**(1), 82–93, DOI: [10.1080/09540105.2012.749220](https://doi.org/10.1080/09540105.2012.749220).
- 7 N. K. Abdelkhalik, E. W. Ghazy and M. M. Abdel-Daim, Pharmacodynamic interaction of Spirulina platensis and deltamethrin in freshwater fish Nile tilapia, *Oreochromis niloticus*: impact on lipid peroxidation and oxidative stress, *Environ. Sci. Pollut. Res.*, 2015, **22**, 3023–3031, DOI: [10.1007/S11356-014-3578](https://doi.org/10.1007/S11356-014-3578).
- 8 M. Wang, H. Kang, D. Xu, C. Wang, S. Liu and X. Hu, Label-free impedimetric immunosensor for sensitive detection of fenvalerate in tea, *Food Chem.*, 2013, **141**, 84–90, DOI: [10.1016/J.FOODCHEM.2013.02.098](https://doi.org/10.1016/J.FOODCHEM.2013.02.098).
- 9 F. A. Guardiola, P. González-Párraga, J. Meseguer, A. Cuesta and M. A. Esteban, Modulatory effects of deltamethrin-exposure on the immune status, metabolism and oxidative stress in gilthead seabream (*Sparus aurata* L.), *Fish Shellfish Immunol.*, 2014, **36**(1), 120–129, DOI: [10.1016/J.FSI.2013.10.020](https://doi.org/10.1016/J.FSI.2013.10.020).
- 10 S. Singh, A. Mukherjee, D. K. Jaiswal, A. P. de Araujo Pereira, R. Prasad, M. Sharma and J. P. Verma, Advances and future prospects of pyrethroids: Toxicity and microbial degradation, *Sci. Total Environ.*, 2022, **829**, 154561, DOI: [10.1016/J.SCITOTENV.2022.154561](https://doi.org/10.1016/J.SCITOTENV.2022.154561).
- 11 M. A. Farajzadeh, L. Khoshmaram and A. A. A. Nabil, Determination of pyrethroid pesticides residues in vegetable oils using liquid–liquid extraction and dispersive liquid–liquid microextraction followed by gas chromatography–flame ionization detection, *J. Food Compos. Anal.*, 2014, **34**, 128–135, DOI: [10.1016/J.JFCA.2014.03.004](https://doi.org/10.1016/J.JFCA.2014.03.004).
- 12 D. B. Martínez, P. P. Vázquez, M. M. Galera and M. G. García, Determination of pyrethroid insecticides in vegetables with liquid chromatography using detection by electrospray mass spectrometry, *Chromatogr.*, 2006, **63**, 487–491, DOI: [10.1365/S10337-006-0777-Y](https://doi.org/10.1365/S10337-006-0777-Y).
- 13 S. M. Shivanoor and M. David, Reversal of deltamethrin-induced oxidative damage in rat neural tissues by turmeric-diet: Fourier transform-infrared and biochemical investigation, *J. Basic Appl. Zool.*, 2016, **77**, 56–68, DOI: [10.1016/J.JOBAZ.2016.10.003](https://doi.org/10.1016/J.JOBAZ.2016.10.003).
- 14 K. R. Kranthi, M. Davis, C. D. Mayee, D. A. Russell, R. M. Shukla, U. Satija and S. Kranthi, Development of a colloidal-gold based lateral-flow immunoassay kit for 'quality-control' assessment of pyrethroid and endosulfan formulations in a novel single strip format, *Crop Prot.*, 2009, **28**(5), 428–434, DOI: [10.1016/J.CROPRO.2009.01.003](https://doi.org/10.1016/J.CROPRO.2009.01.003).
- 15 X. Jin, P. Guo, P. Guan, S. Wang, Y. Lei and G. Wang, The fabrication of paper separation channel based SERS substrate and its recyclable separation and detection of pesticides, *Spectrochim. Acta, Part A*, 2020, **240**, 118561, DOI: [10.1016/J.SAA.2020.118561](https://doi.org/10.1016/J.SAA.2020.118561).
- 16 R. Umapathi, S. Sonwal, M. J. Lee, G. M. Rani, E. S. Lee, T. J. Jeon and Y. S. Huh, Colorimetric based on-site sensing strategies for the rapid detection of pesticides in agricultural foods: New horizons, perspectives, and challenges, *Coord. Chem. Rev.*, 2021, **446**, 214061, DOI: [10.1016/J.CCR.2021.214061](https://doi.org/10.1016/J.CCR.2021.214061).
- 17 S. K. Kailasa, S. Ha, S. H. Baek, S. Kim, K. Kwak and T. J. Park, Tuning of carbon dots emission color for sensing of Fe<sup>3+</sup> ion and bioimaging applications, *Mater. Sci. Eng. C*, 2019, **98**, 834–842, DOI: [10.1016/J.MSEC.2019.01.002](https://doi.org/10.1016/J.MSEC.2019.01.002).
- 18 X. T. Zheng, A. Ananthanarayanan, K. Q. Luo and P. Chen, Glowing graphene quantum dots and carbon dots: properties, syntheses, and biological applications, *Small*, 2015, **11**(14), 1620–1636, DOI: [10.1002/SMLL.201402648](https://doi.org/10.1002/SMLL.201402648).
- 19 M. Zulfajri, H. N. Abdelhamid, S. Sudewi, S. Dayalan, A. Rasool, A. Habib and G. G. Huang, Plant part-derived carbon dots for biosensing, *Biosens.*, 2020, **10**(6), 68, DOI: [10.3390/bios10060068](https://doi.org/10.3390/bios10060068).
- 20 H. Wu, R. Xie, Y. Hao, J. Pang, H. Gao, F. Qu, M. Tian, C. Guo, B. Mao and F. Chai, Portable smartphone-integrated AuAg nanoclusters electrospun membranes for multivariate fluorescent sensing of Hg<sup>2+</sup>, Cu<sup>2+</sup>, and l-histidine in water and food samples, *Food Chem.*, 2023, **418**, 135961, DOI: [10.1016/j.foodchem.2023.135961](https://doi.org/10.1016/j.foodchem.2023.135961).
- 21 G. N. Vajubhai, P. Chetti and S. K. Kailasa, Perovskite Quantum Dots for Fluorescence Turn-Off Detection of the Clodinafop Pesticide in Food Samples via Liquid–Liquid Microextraction, *ACS Appl. Nano Mater.*, 2022, **5**(12), 18220–18228, DOI: [10.1021/acsanm.2c04089](https://doi.org/10.1021/acsanm.2c04089).



- 22 J. V. Rohit and S. K. Kailasa, 5-Sulfo anthranilic acid dithiocarbamate functionalized silver nanoparticles as a colorimetric probe for the simple and selective detection of tricyclazole fungicide in rice samples, *Anal. Methods*, 2014, **6**(15), 5934–5941, DOI: [10.1039/C3AY42092B](https://doi.org/10.1039/C3AY42092B).
- 23 Z. Wang, Y. Huang, D. Wang, L. Sun, C. Dong, L. Fang and A. Wu, A rapid colorimetric method for the detection of deltamethrin based on gold nanoparticles modified with 2-mercapto-6-nitrobenzothiazole, *Anal. Methods*, 2018, **10**, 1774–1780, DOI: [10.1039/C8AY00137E](https://doi.org/10.1039/C8AY00137E).
- 24 H. Qian, Q. Yang, Y. Qu, Z. Ju, W. Zhou and H. Gao, Hydrophobic deep eutectic solvents based membrane emulsification-assisted liquid-phase microextraction method for determination of pyrethroids in tea beverages, *J. Chromatogr. A*, 2020, **1623**, 461204, DOI: [10.1016/J.CHROMA.2020.461204](https://doi.org/10.1016/J.CHROMA.2020.461204).
- 25 T. Guo, C. Wang, H. Zhou, Y. Zhang and L. Ma, A multifunctional near-infrared fluorescent sensing material based on core-shell upconversion nanoparticles@magnetic nanoparticles and molecularly imprinted polymers for detection of deltamethrin, *Microchim. Acta*, 2021, **188**, 1–8, DOI: [10.1007/S00604-021-04811-3/FIGURES/5](https://doi.org/10.1007/S00604-021-04811-3/FIGURES/5).
- 26 Y. Song, R. Xie, M. Tian, B. Mao and F. Chai, Controllable synthesis of bifunctional magnetic carbon dots for rapid fluorescent detection and reversible removal of Hg<sup>2+</sup>, *J. Hazard. Mater.*, 2023, **457**, 131683, DOI: [10.1016/j.jhazmat.2023.131683](https://doi.org/10.1016/j.jhazmat.2023.131683).
- 27 H. N. Abdelhamid, Carbon dots-based fluorescence spectroscopy for metal ion sensing, in *Carbon Dots in Analytical Chemistry*, Elsevier, 2023, pp. 87–96. DOI: [10.1016/B978-0-323-98350-1.00025-6](https://doi.org/10.1016/B978-0-323-98350-1.00025-6).
- 28 V. F. Yusuf, S. V. Atulbhai, B. Swapna, N. I. Malek and S. K. Kailasa, Recent developments in carbon dot-based green analytical methods: new opportunities in fluorescence assays of pesticides, drugs and biomolecules, *New J. Chem.*, 2022, **46**(30), 14287–14308, DOI: [10.1039/D2NJ01401G](https://doi.org/10.1039/D2NJ01401G).
- 29 T. C. Wareing, P. Gentile and A. N. Phan, Biomass-based carbon dots: current development and future perspectives, *ACS Nano*, 2021, **15**(10), 15471–15501, DOI: [10.1021/acsnano.1c03886](https://doi.org/10.1021/acsnano.1c03886).
- 30 J. V. Rohit, V. N. Mehta, A. B. Patel, H. Tabasum, and G. Spolia, Carbon dots-based fluorescence spectrometry for pesticides sensing, in *Carbon Dots in Analytical Chemistry*, Elsevier, 2023, pp. 97–108, DOI: [10.1016/B978-0-323-98350-1.00020-7](https://doi.org/10.1016/B978-0-323-98350-1.00020-7).
- 31 N. Z. Rani, K. Husain and E. Kumolosasi, Moringa genus: a review of phytochemistry and pharmacology, *Front. Pharmacol.*, 2018, **9**, 108, DOI: [10.3389/FPHAR.2018.00108/BIBTEX](https://doi.org/10.3389/FPHAR.2018.00108/BIBTEX).
- 32 D. A. Gupta, M. L. Desai, N. I. Malek and S. K. Kailasa, Fluorescence detection of Fe<sup>3+</sup> ion using ultra-small fluorescent carbon dots derived from pineapple (*Ananas comosus*): Development of miniaturized analytical method, *J. Mol. Struct.*, 2020, **1216**, 128343, DOI: [10.1016/j.molstruc.2020.128343](https://doi.org/10.1016/j.molstruc.2020.128343).
- 33 J. R. Bhamore, S. Jha, T. J. Park and S. K. Kailasa, Green synthesis of multi-color emissive carbon dots from Manilkara zapota fruits for bioimaging of bacterial and fungal cells, *J. Photochem. Photobiol., B*, 2019, **191**, 150–155, DOI: [10.1016/J.JPHOTOBIO.2018.12.023](https://doi.org/10.1016/J.JPHOTOBIO.2018.12.023).
- 34 H. Yan, B. Zhang, Y. Zhang, R. Su, P. Li and W. Su, Fluorescent carbon dot-curcumin nanocomposites for remarkable antibacterial activity with synergistic photodynamic and photothermal abilities, *ACS Appl. Bio Mater.*, 2021, **4**, 6703–6718, DOI: [10.1021/ACSABM.1C00377](https://doi.org/10.1021/ACSABM.1C00377).
- 35 B. Peng, Y. Xu, K. Liu, X. Wang and F. M. Mulder, High-performance and low-cost sodium-ion anode based on a facile black phosphorus-carbon nanocomposite, *ChemElectroChem*, 2017, **4**, 2140–2144, DOI: [10.1002/CELC.201700345](https://doi.org/10.1002/CELC.201700345).
- 36 C. Ferrer, M. J. Gómez, J. F. García-Reyes, I. Ferrer, E. M. Thurman and A. R. Fernández-Alba, Determination of pesticide residues in olives and olive oil by matrix solid-phase dispersion followed by gas chromatography/mass spectrometry and liquid chromatography/tandem mass spectrometry, *J. Chromatogr. A*, 2005, **1069**, 183–194, DOI: [10.1016/J.CHROMA.2005.02.015](https://doi.org/10.1016/J.CHROMA.2005.02.015).
- 37 Z. Wang, Y. Huang, D. Wang, L. Sun, C. Dong, L. Fang and A. Wu, A rapid colorimetric method for the detection of deltamethrin based on gold nanoparticles modified with 2-mercapto-6-nitrobenzothiazole, *Anal. Methods*, 2018, **10**, 1774–1780, DOI: [10.1039/C8AY00137E](https://doi.org/10.1039/C8AY00137E).
- 38 H. Qian, Q. Yang, Y. Qu, Z. Ju, W. Zhou and H. Gao, Hydrophobic deep eutectic solvents based membrane emulsification-assisted liquid-phase microextraction method for determination of pyrethroids in tea beverages, *J. Chromatogr. A*, 2020, **1623**, 461204, DOI: [10.1016/J.CHROMA.2020.461204](https://doi.org/10.1016/J.CHROMA.2020.461204).
- 39 T. Guo, C. Wang, H. Zhou, Y. Zhang and L. Ma, A multifunctional near-infrared fluorescent sensing material based on core-shell upconversion nanoparticles@magnetic nanoparticles and molecularly imprinted polymers for detection of deltamethrin, *Microchim. Acta*, 2021, **188**, 1–8, DOI: [10.1007/S00604-021-04811-3/FIGURES/5](https://doi.org/10.1007/S00604-021-04811-3/FIGURES/5).
- 40 S. Ge, J. Lu, L. Ge, M. Yan and J. Yu, Development of a novel deltamethrin sensor based on molecularly imprinted silica nanospheres embedded CdTe quantum dots, *Spectrochim. Acta, Part A*, 2011, **79**, 1704–1709, DOI: [10.1016/J.SAA.2011.05.040](https://doi.org/10.1016/J.SAA.2011.05.040).
- 41 I. Al Yahyai, J. Hassanzadeh and H. A. Al-Lawati, A novel and selective multi-emission chemiluminescence system for the quantification of deltamethrin in food samples, *Sens. Actuators, B*, 2021, **327**, 128927, DOI: [10.1016/j.snb.2020.128927](https://doi.org/10.1016/j.snb.2020.128927).
- 42 M. Azimi, J. L. Manzoori, M. Amjadi and J. Abolhasani, Determination of Deltamethrin in Water Samples Using Sulfur and Nitrogen Co-Doped Carbon Quantum Dots as a Chemiluminescence Probe, *J. Anal. Chem.*, 2021, **76**, 1217–1224, DOI: [10.1134/S1061934821100026](https://doi.org/10.1134/S1061934821100026).
- 43 J. R. Bhamore, S. Jha, R. K. Singhal, Z. V. P. Murthy and S. K. Kailasa, Amylase protected gold nanoclusters as



- chemo- and bio-sensor for nanomolar detection of deltamethrin and glutathione, *Sens. Actuators, B*, 2019, **281**, 812–820, DOI: [10.1016/j.snb.2018.11.001](https://doi.org/10.1016/j.snb.2018.11.001).
- 44 W. Deng, L. Yu, X. Li, J. Chen, X. Wang, Z. Deng and Y. Xiao, Hexafluoroisopropanol-based hydrophobic deep eutectic solvents for dispersive liquid-liquid microextraction of pyrethroids in tea beverages and fruit juices, *Food Chem.*, 2019, **274**, 891–899, DOI: [10.1016/J.FOODCHEM.2018.09.048](https://doi.org/10.1016/J.FOODCHEM.2018.09.048).
- 45 V. Nardelli, F. Casamassima, G. Gesualdo, D. Li, W. M. Marchesiello, D. Nardiello and M. Quinto, Sensitive screening method for determination of pyrethroids in chicken eggs and various meat samples by gas chromatography and electron capture detection, *J. Agric. Food Chem.*, 2018, **66**, 10267–10273, DOI: [10.1021/ACS.JAFC](https://doi.org/10.1021/ACS.JAFC).
- 46 L. Tian, C. Kong, C. Fang, X. Lou, F. Han, Y. Shi and Y. Cai, Research of detection and quantitative method of cypermethrin, fenvalerate and deltamethrin residues in sediment by gas chromatography, *IOP Conf. Ser.: Earth Environ. Sci.*, 2019, **233**, 042012, DOI: [10.1088/1755-1315/233/4/042012](https://doi.org/10.1088/1755-1315/233/4/042012).
- 47 S. Zhao, J. Lei, D. Huo, C. Hou, P. Yang, J. Huang and X. Luo, A laser-induced fluorescent detector for pesticide residue detection based on the spectral recognition method, *Anal. Methods*, 2018, **10**(46), 5507–5515, DOI: [10.1039/C8AY02067A](https://doi.org/10.1039/C8AY02067A).
- 48 W. Wang and H. Ouyang, Luminol-reduced Au nanoparticles-based dual-signal immunochromatographic test strip for pesticide residues, *Microchem. J.*, 2019, **149**, 104055, DOI: [10.1016/j.microc.2019.104055](https://doi.org/10.1016/j.microc.2019.104055).
- 49 Y. Wang, D. Zang, S. Ge, L. Ge, J. Yu and M. Yan, A novel microfluidic origami photoelectrochemical sensor based on CdTe quantum dots modified molecularly imprinted polymer and its highly selective detection of S-fenvalerate, *Electrochim. Acta*, 2013, **107**, 147–154, DOI: [10.1016/j.electacta.2013.05.154](https://doi.org/10.1016/j.electacta.2013.05.154).
- 50 H. Li, Y. Wang, Y. Li, J. Zhang, Y. Qiao, Q. Wang and G. Che, Fabrication of pollutant-resistance SERS imprinted sensors based on SiO<sub>2</sub>@ TiO<sub>2</sub>@ Ag composites for selective detection of pyrethroids in water, *J. Phys. Chem. Solids*, 2020, **138**, 109254, DOI: [10.1016/J.JPCS.2019.109254](https://doi.org/10.1016/J.JPCS.2019.109254).

